

# Binding of Hisactophilin I and II to Lipid Membranes Is Controlled by a pH-Dependent Myristoyl–Histidine Switch<sup>†</sup>

Frank Hanakam,<sup>‡</sup> Günther Gerisch,<sup>‡</sup> Sandra Lotz,<sup>§</sup> Thomas Alt,<sup>§</sup> and Anna Seelig<sup>\*,§</sup>

Max-Planck-Institut für Biochemie, D-82152 Martinsried, Germany, and Department of Biophysical Chemistry, Biocenter of the University of Basel, Klingelbergstrasse 70, CH-4056 Basel, Switzerland

Received April 2, 1996; Revised Manuscript Received June 11, 1996<sup>®</sup>

**ABSTRACT:** The interaction of the two N-terminally myristoylated isoforms of *Dictyostelium* hisactophilin with lipid model membranes was investigated by means of the monolayer expansion method and high-sensitivity titration calorimetry. The two isoforms, hisactophilin I and hisactophilin II, were found to insert with their N-terminal myristoyl residue into an electrically neutral POPC monolayer corresponding in its lateral packing density to that of a lipid bilayer. The partition coefficient for this insertion process was  $K_p = (1.1 \pm 0.2) \times 10^4 \text{ M}^{-1}$ . The area requirement of the protein in the lipid membrane was estimated as  $44 \pm 6 \text{ \AA}^2$  which corresponds to the cross sectional area of the myristoyl moiety with an additional small contribution from amino acid side chains. The interaction of hisactophilin I (hisactophilin II) with negatively charged membrane surfaces is modulated in a pH-dependent manner by charged amino acid residues clustered around the myristoyl moiety. The electrostatic binding site consists of three lysine (one arginine and two lysine), seven (nine) histidine, and four (four) glutamic acid residues and has an isoelectric point of 6.9 (7.1). For small unilamellar POPC/POPG (75/25 mole/mole) vesicles, an apparent binding constant,  $K_{app} = (8 \pm 1) \times 10^5 \text{ M}^{-1}$ , was measured at pH 6.0 by means of high-sensitivity titration calorimetry. Electrostatic interactions hence increase the binding constant by about 2 orders of magnitude compared to hydrophobic binding alone. With increasing pH, the electrostatic attraction decreases and turns into an electrostatic repulsion at  $\text{pH} > 7.0 \pm 0.1$ . The area occupied by the cluster of charged residues constituting the membrane binding region was  $280 \pm 20 \text{ \AA}^2$  as derived from monolayer measurements in close agreement with molecular modeling data derived from the NMR structure of hisactophilin I [Habazettl et al. (1992) *Nature* 359, 855–858].

Hisactophilins are proteins which have been implicated in coupling the actin skeleton to plasma membranes in the highly motile amoeboid cells of *Dictyostelium discoideum* (Scheel et al., 1989; Behrisch et al., 1995; Hanakam et al., 1996). Two isoforms, HsI<sup>1</sup> (13.5 kDa) and HsII (13.7 kDa), consisting of 118 amino acid residues each were isolated (Hanakam et al., 1995). They show 84% identity and 91% similarity in their amino acid sequence. The most distinctive feature is their high histidine content which is 26% for HsI and 30% for HsII. The three-dimensional structure of HsI expressed in *Escherichia coli* has been resolved by NMR (Habazettl et al., 1992), revealing 12 antiparallel  $\beta$ -strands arranged in three subunits. The first and fourth  $\beta$ -strands of each unit form a  $\beta$ -sheet which is grouped around a 3-fold axis of symmetry in the form of a  $\beta$ -barrel. The N- and the C-terminus are located close to the central axis, in a way that their charged residues cluster at the protein surface. The side chains of most of the hydrophobic residues are oriented to the inside of the barrel. The tightly packed  $\beta$ -strands are

connected by turns and loops which show greater flexibility and carry all glycine and most of the histidine residues.

Both hisactophilin isoforms isolated from *D. discoideum* cells are myristoylated at their N-terminal glycine (Hanakam et al., 1995), and they thus belong to the still growing number of myristoylated proteins detected in the cytosol and in subcellular compartments of eukaryotic cells (Magee & Courtneidge, 1985; Blenis & Resh, 1992). The myristoyl moiety has been suggested to have different functions [cf. Vergères et al. (1995)]. Its best investigated function is to mediate membrane binding [Peitsch & McLaughlin, 1993; Vergères et al., 1995; for review, see McLaughlin and Aderem, (1995)]. The myristoyl moiety alone, however, barely provides enough hydrophobic energy to attach a protein to a phospholipid membrane (Peitsch & McLaughlin, 1993). The hydrophobic anchoring via the myristoyl chain is therefore often reinforced by additional hydrophobic and/or electrostatic interactions. An additional palmitoyl or myristoyl chain is found in several members of the G-protein  $\alpha$ -subunits family (Bigay et al., 1994), whereas a cluster of basic amino acid residues enhances binding in the protein kinase C substrate, MARCKS (Kim et al., 1994a), and the protein tyrosine kinase, Src (Buser et al., 1994; Sigal et al., 1994). Binding of these proteins to negatively charged membranes is reversed by phosphorylation which increases the negative charge of the protein and therefore induces electrostatic repulsion (Kim et al., 1994a,b). The subtle balance between hydrophobic and electrostatic attractive and repulsive forces regulated by phosphorylation provides the

<sup>†</sup> Supported by the Swiss National Science Foundation Grant 31.42 058. 94.

\* Corresponding author. Fax: +41-61-267-2189.

<sup>‡</sup> Max-Planck-Institut für Biochemie.

<sup>§</sup> Biocenter of the University of Basel.

<sup>®</sup> Abstract published in *Advance ACS Abstracts*, August 1, 1996.

<sup>1</sup> Abbreviations: HsI and HsII, isoforms of hisactophilin; POPC, 1-palmitoyl-2-oleoyl-*sn*-glycero-3-phosphocholine; POPG, 1-palmitoyl-2-oleoyl-*sn*-glycero-3-phosphoglycerol; Src, N-terminal motif of the tyrosine kinase v-Src; MARCKS, myristoylated alanine rich C kinase substrate; CD, circular dichroism; NMR, nuclear magnetic resonance spectroscopy.

basis for the “myristoyl-electrostatic switch mechanism” described by McLaughlin and Aderem (1995).

In *D. discoideum*, the switch mechanism responsible for the reversible binding of hisactophilins to the plasma membrane is most probably modulated by cytoplasmic pH changes and not by phosphorylation. An equilibrium between protein in the cytosol and protein bound to the plasma membrane has been observed for HsI and HsII (Hanakam et al., 1995). The equilibrium is shifted in the living cell toward the membrane-bound state by lowering the cytoplasmic pH (Hanakam et al., 1996). Under physiological conditions, intracellular pH changes occur in *D. discoideum*, and these changes have functional consequences. An intracellular pH increase was observed in response to cAMP pulses, generated as chemotactic signals by aggregating cells of this organism (Van Lookeren Campagne et al., 1989). Alterations of intracellular pH have further been shown to regulate the speed of cell locomotion (Van Duijn & Inouye, 1991) and to control cell differentiation (Gross et al., 1983).

At low ionic strength, the binding of hisactophilin to negatively charged lipid monolayers has been reported to be purely electrostatic (Behrisch et al., 1995). The aim of the present work was to investigate the pH-dependent binding of hisactophilin to lipid model membranes at physiological salt concentrations where electrostatic interactions are reduced. To distinguish between the contribution of hydrophobic and electrostatic interactions, we measured the binding of the two myristoylated isoforms, HsI and HsII, to neutral and negatively charged lipid model membranes, the latter containing 25% negatively charged phospholipids. As model membranes, we used lipid monolayers and small unilamellar vesicles. Binding was measured by means of the monolayer expansion method at constant surface pressure (Seelig et al., 1996) and by high-sensitivity titration calorimetry (Wisemann et al., 1989). We demonstrate that the binding of both hisactophilin isoforms to negatively charged model membranes is due to a synergism of hydrophobic and electrostatic interactions. The hydrophobic interaction arises from the insertion of the myristoyl chain into the lipid membrane interior. The electrostatic interaction with a negatively charged membrane surface is due to N- and C-terminal cationic and anionic amino acid residues clustered around Gly<sup>2</sup> to which the myristoyl chain is bound. This cluster is rich in histidines and therefore switches its net charge from cationic to anionic at pH  $7.0 \pm 0.1$ .

## MATERIALS AND METHODS

**Purification of Hisactophilin I and II.** Purification of HsI and HsII from the cytosolic fraction of *D. discoideum* was performed as described by Hanakam et al. (1995). The purified protein was dialyzed against Tris buffer [50 mM Tris/HCl (pH 8.8), 154 mM NaCl, 1 mM DTT, and 0.02% NaN<sub>3</sub>]. The hisactophilin concentrations were quantified by HPLC. The relative areas were calibrated by means of a hisactophilin standard solution of known concentration, determined by amino acid analysis. The two isoforms HsI and HsII could be separated under isocratic conditions and could therefore be quantified by a comparison of the relative areas of the HPLC chromatogram (Hanakam et al., 1995).

**Lipids.** 1-Palmitoyl-2-oleoyl-*sn*-glycero-3-phosphocholine (POPC) and 1-palmitoyl-2-oleoyl-*sn*-glycero-3-phosphoglyc-

erol (POPG) were purchased from Avanti Polar Lipids (Birmingham, AL) and were used without further purification.

**Vesicle Preparation.** For titration calorimetry, small unilamellar POPC/POPG (75/25 mole/mole) vesicles were prepared by dissolving an appropriate amount of lipid in chloroform/methanol. The solvent was evaporated under a stream of nitrogen, and the lipid was dried overnight under vacuum. Buffer was added to the dry lipid film, and the suspension was vortexed until the suspension appeared almost homogeneous. The lipid dispersion was then sonified under nitrogen for 20–40 min (at 10 °C) until an almost clear solution was obtained. Metal debris from the titanium tip was removed by centrifugation in an Eppendorf centrifuge for 10 min. The sonified vesicles had a diameter of  $250 \pm 30$  Å as determined by electron microscopy (N. Taschner, unpublished results).

**Circular Dichroism Measurements.** Circular dichroism (CD) spectra were measured with a Jasco J720 spectropolarimeter. All measurements were performed at ambient temperature. The path length of the cell was 1 mm. All spectra were corrected by subtracting the buffer baseline. Results were plotted as mean residue ellipticity,  $\Theta$ , in units of deg cm<sup>2</sup> dmol<sup>−1</sup>. Estimations of the percentage of secondary structures were obtained from a computer simulation based on the reference spectra of Yang et al. (1986).

**Monolayer Measurements.** A round Teflon trough designed by Fromherz (1975) (type RCM 2-T, Mayer Feintech, Göttingen, FRG) with a total area of 362 cm<sup>2</sup> divided into eight compartments was used. The trough was covered by a Plexiglas hood in order to keep humidity constant. The surface pressure,  $\pi = \gamma_0 - \gamma$ , where  $\gamma_0$  is the surface tension of the pure buffer and  $\gamma$  the surface tension of the peptide solution, was monitored by means of a Whatman no. 1 filter paper, connected to a Wilhelmy balance. Measurements were performed at  $21 \pm 1$  °C.

For insertion experiments, two compartments of the trough were used, containing together 40 mL of buffer solution. The monolayer was formed by depositing a drop of lipid dissolved in hexane/ethanol (9/1, v/v) on the buffer surface between a fixed and a movable barrier and was then left to stabilize for about 15 min. The initial area,  $A$  (typically around 50 cm<sup>2</sup>), contained  $n_L$  lipid molecules of an area  $A_L$ . Protein ( $\sim 1$  mg/mL) dissolved in buffer was injected with a Hamilton syringe into the buffer subphase and was left to equilibrate between the aqueous and the lipid phase. The surface pressure,  $\pi$ , was kept constant during the insertion experiments by means of an electronic feedback system. The insertion of  $n_P$  protein molecules with an insertion area of  $A_P$  into the monolayer thus gave rise to an area expansion,  $\Delta A$ . The mole fraction of protein in the monolayer is defined as  $X_b = n_P/n_L$  and can be evaluated from the relative area increase,  $\Delta A/A$ , provided  $A_L$  and  $A_P$  are known (see below) (Seelig, 1987)

$$X_b = n_P/n_L = (\Delta A/A)(A_L/A_P) \quad (1)$$

As a first approximation, the binding to the lipid membrane can be described in terms of a simple partition equilibrium

$$X_b = K_{app} C_{eq} \quad (2)$$

where  $K_{app}$  is the apparent binding constant [see Seelig (1992)].

In order to penetrate into a lipid monolayer with a lateral pressure  $\pi$ , a protein molecule has to perform the work,  $\Delta W = \pi A_p$ , where the penetration area,  $A_p$ , is the area which the protein occupies in the lipid monolayer. The free energy of penetration will therefore vary with the monolayer surface pressure,  $\pi$ . According to Boguslavsky et al. (1994), the variation of the binding constant with pressure is given by

$$K = K_0 e^{-\pi A_p / kT} \quad (3)$$

Combining eqs 1 and 3 yields the surface pressure dependence of the relative area increase,  $\Delta A/A$ , at constant  $C_{eq}$  under the assumption of a constant penetration area,  $A_p$ , and a constant lipid area,  $A_L$ <sup>2</sup>

$$\Delta A/A = (A_p/A_L) K_0 C_{eq} e^{-\pi A_p / kT} \approx \text{constant} e^{-\pi A_p / kT} \quad (4)$$

The measured pressure dependence of the  $\Delta A/A$  curves can then be used to determine the penetration area,  $A_p$ .

**High-Sensitivity Titration Calorimetry.** Heats of reaction were measured with a Microcal OMEGA titration calorimeter (Microcal, Northampton, MA) as described previously (Wiseman et al., 1989). Solutions were degassed under vacuum prior to use. The calorimeter was calibrated electrically. Measurements were performed at 28 °C. The data were evaluated using software (Origin) developed by MicroCal. The protein used for titration calorimetry was dialyzed against 10 mM Mes buffer at pH 6.0 (0.02% NaN<sub>3</sub>, 1 mM DTT, and 154 mM NaCl). The same buffer was used for vesicle preparation. Before and after dialysis, the protein concentration was measured by CD, using the spectrum of a hisactophilin standard solution with a known concentration as a reference.

**Surface Charge Calculation.** The net charge of the protein was calculated as the sum of the number of positively charged amino acid residues (protonated lysine, arginine, and histidine) minus the number of negatively charged residues (deprotonated tyrosine, cysteine, glutamate, and aspartate) plus the number of protonated amino termini minus the number of carboxyl termini. Any electrostatic interactions within the protein that may perturb ionization were taken into account. For each amino acid of interest, the number of protonated residues was determined by

$$N_p = N_t [H^+] / ([H^+] + K_N)$$

where  $N_p$  is the number of protonated residues,  $N_t$  the total number of residues of a specific amino acid,  $[H^+]$  the hydrogen ion concentration, and  $K_N$  the dissociation constant (Devereux et al., 1984). The following  $pK_N$  values were used: 8.3 (Cys), 3.91 (Asp), 4.25 (Glu), 6.5 (His), 10.79 (Lys), 12.50 (Arg), 10.95 (Tyr), 8.56 (NH<sub>2</sub>), and 3.56 (COOH) (Bull, 1971).

**Molecular Modeling.** Models were developed on a Silicon Graphics workstation using the Insight II 2.3.0 software (Biosym, San Diego, CA). The structural data for HsII were derived from the NMR data of HsI (Habazettl et al., 1992). The amino acids specific for HsII were exchanged in the HsI structure without further energy minimization. A POPC

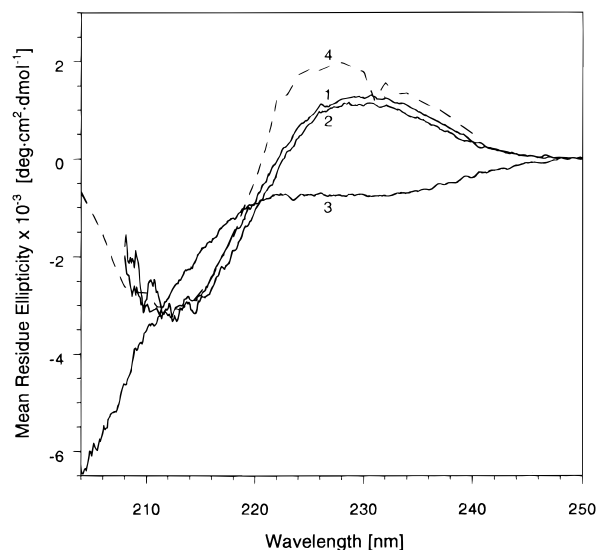


FIGURE 1: CD spectrum of HsI/HsII (50/50 mole/mole) at pH 8 (10 mM Tris) (1), pH 6.0 (10 mM Mes) (2), and pH 3 (10 mM Mes/HCl) (3). All buffers contained 1 mM DTT, 0.02% NaN<sub>3</sub>, and 154 mM NaCl. Protein concentrations were 40  $\mu$ M. The dashed line (4) represents the spectrum simulated on the basis of the structural data obtained by NMR (Habazettl et al., 1992) using the reference spectra of Yang et al. (1986).

bilayer in the liquid crystalline phase was simulated according to Heller et al. (1993).

## RESULTS

**Secondary Structure of Hisactophilins as Monitored by CD.** Figure 1 displays the CD spectra of an equimolar solution of HsI and HsII measured at pH 8.0, 6.0, and 3.0. At pH 8.0 and 6.0, the spectra were practically identical and exhibited a minimum around 212 nm, with a residue ellipticity  $\Theta = -3100$  deg cm<sup>2</sup> dmol<sup>-1</sup>, and a maximum at about 228 nm, with a residue ellipticity  $\Theta = +1200$  deg cm<sup>2</sup> dmol<sup>-1</sup>. The HsI spectrum was simulated with the structural data obtained by NMR (57%  $\beta$ -sheet, 21%  $\beta$ -turn, and 22% random coil) (Habazettl et al., 1992) using the reference spectra of Yang et al. (1986) (dashed line). A perfect fit was obtained below 220 nm, in the region characteristic for the well-defined  $\beta$ -sheet and random coil structures. The spectrum at pH 3.0 shows a minimum below 204 nm, indicating a distinct increase in random coil conformation with a concomitant decrease in  $\beta$ -sheet structures. This spectrum can be fitted with 16%  $\beta$ -sheet, 32%  $\beta$ -turn, and 52% random coil conformation (not shown). Upon realkalinization, refolding was observed (Habazettl et al., 1992).

The spectra of HsI/HsII (80/20 mole/mole) and HsI/HsII (20/80 mole/mole) were identical to the spectra of HsI/HsII (50/50 mole/mole) shown above under the same experimental conditions, suggesting a high similarity of the secondary structures of the two isoforms. At pH 8.0 and a temperature of 6 °C, the secondary structure of hisactophilins was very stable and remained intact over several weeks.

**Relative Area Increase  $\Delta A/A$  Due to Hisactophilin Insertion as a Function of the Monolayer Surface Pressure.** Figure 2A summarizes the insertion measurements of different mixtures of HsI and HsII into POPC and POPC/POPG (75/25 mole/mole) monolayers as a function of the surface pressure,  $\pi$ . Each experimental point corresponds to a new

<sup>2</sup> The assumption of constant areas can be made to a first approximation since  $A_L$  and  $A_p$  change by at most 15% in the pressure range investigated.

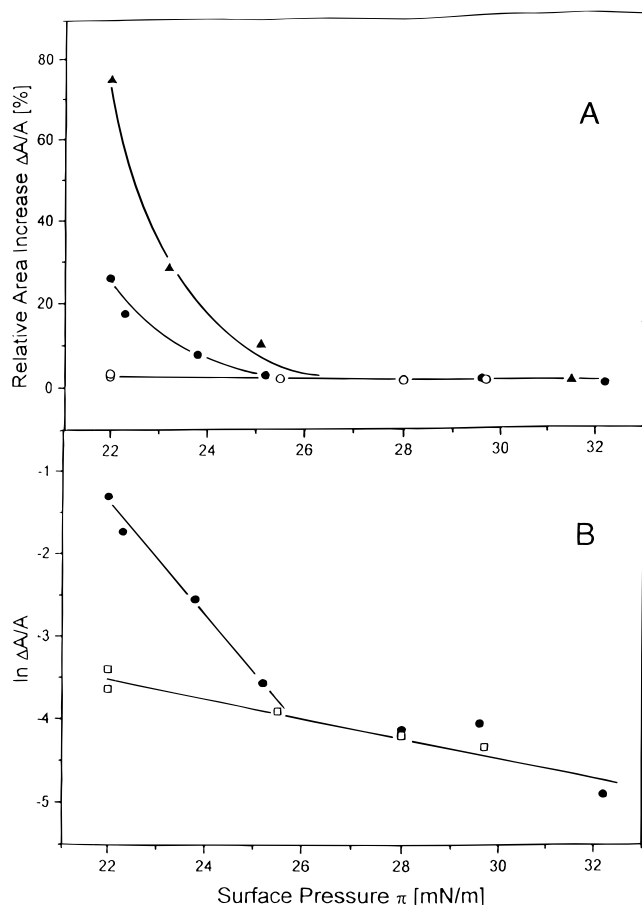


FIGURE 2: (A) Relative area increase,  $\Delta A/A$ , upon penetration of HsI/HsII (20/80 mole/mole) (▲), HsI/HsII (80/20 mole/mole) (●), and HsI/HsII (50/50 mole/mole) (○) as a function of the monolayer surface pressure  $\pi$ . The lipid monolayer consisted of POPC (open symbol) or POPC/POPG (75/25 mole/mole) (closed symbols). Measurements were performed at pH 6.0 (10 mM Pipes, 154 mM NaCl, 1 mM DTT, and 0.02%  $\text{NaN}_3$ ). The protein concentration in the monolayer trough was  $0.73 \mu\text{M}$  in the presence of negatively charged and  $0.95 \mu\text{M}$  in the presence of neutral monolayers, respectively. (B) Semilogarithmic plot of  $\Delta A/A$  as a function of  $\pi$  for HsI/HsII (50/50 mole/mole) in the presence of POPC (○) and for HsI/HsII (80/20 mole/mole) in the presence of POPC/POPG monolayers (●). From the slopes of the straight lines, the penetration areas,  $A_p$ , of the protein were determined.

lipid monolayer with a preset surface pressure. Since the latter was kept constant, penetration of the protein into a lipid layer with the initial area  $A$  gave rise to an area expansion  $\Delta A$ . The relative area increase,  $\Delta A/A$ , due to penetration of HsI/HsII (50/50 mole/mole) into neutral POPC monolayers was small, but still measurable, and showed little dependence on the surface pressure. In contrast, the penetration of HsI/HsII (80/20 mole/mole or 20/80 mole/mole) mixtures into negatively charged POPC/POPG (75/25 mole/mole) monolayers led to a large increase of  $\Delta A/A$ . This increase was highly dependent on the surface pressure,  $\pi$ , of the lipid monolayer. Under identical experimental conditions, HsI/HsII (20/80 mole/mole) mixtures inserted almost twice as strongly as HsI/HsII (80/20 mole/mole), suggesting a stronger electrostatic attraction of HsII to the negatively charged lipid membrane.

According to eq 4, a semilogarithmic plot of  $\Delta A/A$  as a function of the surface pressure,  $\pi$ , should yield a straight line if the protein inserts with a constant area,  $A_p$ . As seen in Figure 2B, this is indeed the case for the hisactophilin

penetration into electrically neutral monolayers. From the slope of the curve, the penetration area,  $A_p$ , was derived as  $44 \pm 6 \text{ \AA}^2$ . For negatively charged monolayers, the semilogarithmic plot of  $\Delta A/A$  versus  $\pi$  is, however, biphasic. From the two slopes, the penetration areas,  $A_{p1} = 280 \pm 20 \text{ \AA}^2$  and  $A_{p2} = 44 \pm 10 \text{ \AA}^2$ , were determined at low and high pressures, respectively.

From Figure 2B, the partition coefficient of hisactophilin for electrically neutral lipid membranes can be estimated. The surface pressure of a lipid bilayer corresponds to that of a lipid monolayer at 32–35 mN/m (Demel et al., 1975; Blume, 1979; Seelig, 1987; Taschner, 1992). From a linear extrapolation of the  $\ln \Delta A/A$  versus  $\pi$  curve in Figure 2B, the relative area increase,  $\Delta A/A$ , at 32 mN/m was determined and was then converted to the mole fraction,  $X_b$ , of protein bound to the monolayer according to eq 1. Using the areas,  $A_L = 65 \text{ \AA}^2$  for lipids (Evans et al., 1987; Taschner, 1992) and  $A_p = 44 \text{ \AA}^2$  for hisactophilin, the partition coefficient  $K_A = X_b/C_{eq}$ , describing the hydrophobic interaction of hisactophilin with a lipid monolayer, corresponding in its lateral packing density to that of a lipid bilayer, was determined as  $(1.1 \pm 0.2) \times 10^4 \text{ M}^{-1}$ . At the low protein concentrations used in these experiments, electrostatic effects can be neglected and the binding can be regarded, to a first approximation, as a pure partitioning reaction.

**Hisactophilin Binding Constant for Negatively Charged Lipid Vesicles Determined at pH 6.0.** The binding of cationic hisactophilin to small unilamellar POPC/POPG (75/25 mole/mole) vesicles, which mimic the negative surface charge density of the inner leaflet of the plasma membrane (Op den Kamp, 1979), was measured by means of high-sensitivity titration calorimetry. The calorimeter cell, with a volume of  $V_{\text{cell}} = 1.278 \text{ mL}$ , contained a  $31 \mu\text{M}$  HsI/HsII (70/30) solution in buffer at pH 6.0. Each peak in the titration experiment shown in Figure 3A corresponds to the injection of  $10 \mu\text{L}$  of sonified POPC/POPG (75/25 mole/mole) vesicles. The lipid concentration was  $26.13 \text{ mg/mL}$ , but only the outer surface of the lipid vesicles (60% of the total lipid) is accessible to proteins. The endothermic heat of reaction decreases with consecutive injections since less and less protein is available for binding. Control experiments in which the same lipid vesicles were injected into buffer without protein showed only small endothermic heats of reaction ( $1\text{--}3 \mu\text{cal}$ ) which were subtracted in the final analysis. The calorimetric binding enthalpy was obtained by integrating the area under each peak. Figure 3B shows the cumulative reaction enthalpy as a function of the number of injections.

The measured heat of reaction,  $\Delta h$ , is related to the amount of bound protein according to Beschiaschvili and Seelig (1992):

$$\Delta h = \Delta H X_b C_L^0 V_{\text{cell}} \quad (5)$$

where  $\Delta H$  is the molar heat of binding of the protein and  $C_L^0$  is the lipid concentration in the cell accessible to the protein (60% of the total lipid concentration). The conventional Scatchard analysis of the binding isotherms led to nonlinear plots indicating a more complex binding behavior than anticipated on the basis of a Langmuir adsorption model. From the initial part of the Scatchard plot, an apparent binding constant  $K_{\text{app}} = (8 \pm 1) \times 10^5 \text{ M}^{-1}$  is obtained. The nonlinearity of the  $X_b/C_{eq}$  versus  $X_b$  curve observed for the

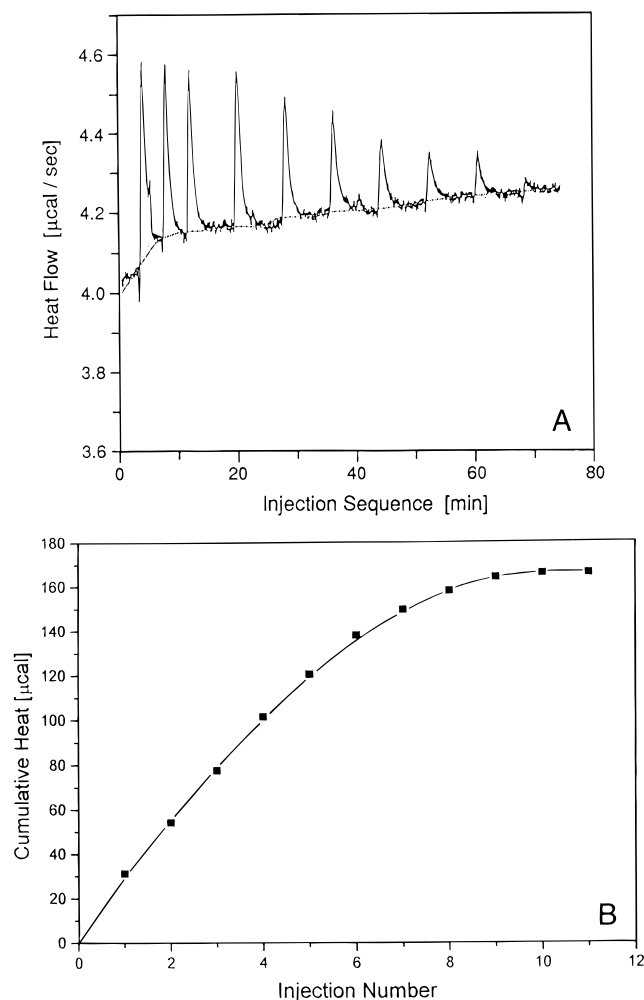


FIGURE 3: (A) Titration calorimetry of HsI/HsII (70/30 mole/mole) with sonified unilamellar vesicles composed of POPG/POPC (25/75 mole/mole) at pH 6.0 (10 mM Mes, 0.02%  $\text{NaN}_3$ , 1 mM DTT, and 154 mM NaCl) and 28 °C. Calorimeter trace for the injection of sonified lipid vesicles (26.13 mg/mL) into protein (31  $\mu\text{M}$ ). (B) Cumulative heat of reaction as a function of the number of injections. The volume of injection was 10  $\mu\text{L}$ .

interaction of cationic hisactophilin with negatively charged lipids is characteristic for electrostatic interactions. It arises from a decrease of the negative surface potential upon binding of the cationic protein. A similar behavior has been described previously for the interaction of cationic peptides with negatively charged membranes (Seelig & Macdonald, 1989; Seelig, 1992).

**pH Dependence of Hisactophilin Binding to Negatively Charged Lipid Monolayers.** At surface pressures relevant for lipid bilayers, the area increase of negatively charged lipid monolayers upon interaction of hisactophilins is small and can be attributed to the insertion of the myristoyl moiety (see Discussion). However, a strong interaction of the charged residues constituting the membrane contact region is observed at low surface pressures ( $\pi < 28 \text{ mN/m}$ ), leading to a distinct increase in the monolayer area (Figure 2). Since the pH variation of the electric charge of hisactophilins is independent of the monolayer packing density, the POPG/POPC monolayer at low surface pressures is a convenient model system to monitor the electrostatic properties of the protein contact region.

As shown in Figure 4, the relative area increase,  $\Delta A/A$ , due to the insertion of HsI/HsII (50/50 mole/mole) into

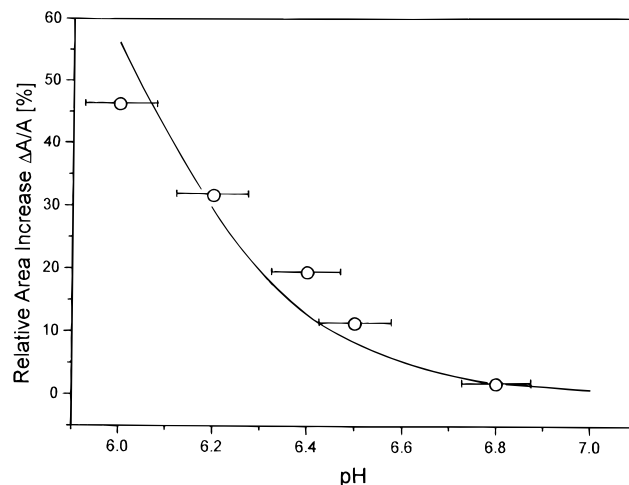


FIGURE 4: Relative area increase,  $\Delta A/A$ , due to HsI/HsII (50/50 mole/mole) (0.95  $\mu\text{M}$ ) insertion into a POPC/POPG monolayer (75/25 mole/mole) as a function of the pH of the buffer solution. All buffers contained 0.02%  $\text{NaN}_3$ , 1 mM DTT, and 154 mM NaCl. For each pH value, a new monolayer was spread on a new buffer solution. The solid line corresponds to a calculated curve of the form  $\Delta A/A = K_A(A_P/A_L)C_{eq}e^{-\Psi_0 z_P F_0 / kT}$ , where  $K_A$  is the hydrophobic binding constant,  $A_P$  the penetration area of the protein which was assumed to decrease linearly from 280 to 44  $\text{\AA}^2$  in the range of pH 6–7,  $A_L$  the area of the lipid,  $C_{eq}$  the equilibrium concentration of the protein,  $\Psi_0$  the surface potential of the negatively charged monolayer (–27 mV),  $z_P$  the effective charge of the binding region ( $z_P = 0.7z_{net}$ ),  $z_{net}$  the net charge of the binding region of the protein (cf. Figure 7),  $F_0$  the Faraday constant, and  $RT$  the thermal energy [cf. Seelig (1992)].

POPC/POPG (75/25 mole/mole) monolayers was measured as a function of the pH in the pH range of 6.0–7.0. At low pH, where the hisactophilins are in their cationic form, a large relative area increase is observed. Increasing the pH decreases the positive charge of the molecule and concomitantly the extent of insertion into the lipid monolayer. An extrapolation of the experimental  $\Delta A/A$  versus pH curve to pH 7.0 (Figure 4) yields the same mole fraction,  $X_b$ , of bound protein, as observed for electrically neutral monolayers. This suggests that the isoelectric point of HsI/HsII (50/50 mole/mole) is reached at  $\text{pH} = 7.0 \pm 0.1$ .

**Surface Charge of Hisactophilins and of Their Membrane Contact Regions.** A molecular model of HsI and HsII was built on the basis of the NMR data for the structure of recombinant, unmyristoylated HsI (Habazettl et al., 1992). Since N-terminal myristoylation has been established by biochemical analysis (Hanakam et al., 1995), an extended myristoyl chain was attached at Gly<sup>2</sup>. The electrostatic fields of HsI and HsII were calculated on the basis of the theory of Poisson–Boltzmann (see Materials and Methods) and are displayed as isocharge surfaces of  $+1kT/e$  (blue areas) and  $-1kT/e$  (red areas), where  $kT$  is the thermal energy and  $e$  the elementary charge. The electrostatic fields of the two isoforms resemble each other in their shape. At pH 6.5, the positive charge dominates over the entire protein surface (Figure 5). Around pH 7.0, the positive charge is reduced due to deprotonation of the histidine residues, and at pH 7.5, the negative surface charge predominates. For HsI, the negative surface charge is slightly higher than for HsII at a given pH, in agreement with the lower isoelectric point of HsI (see below).

The amino acid residues constituting the membrane contact region were deduced from the models of HsI (HsII) (Figure

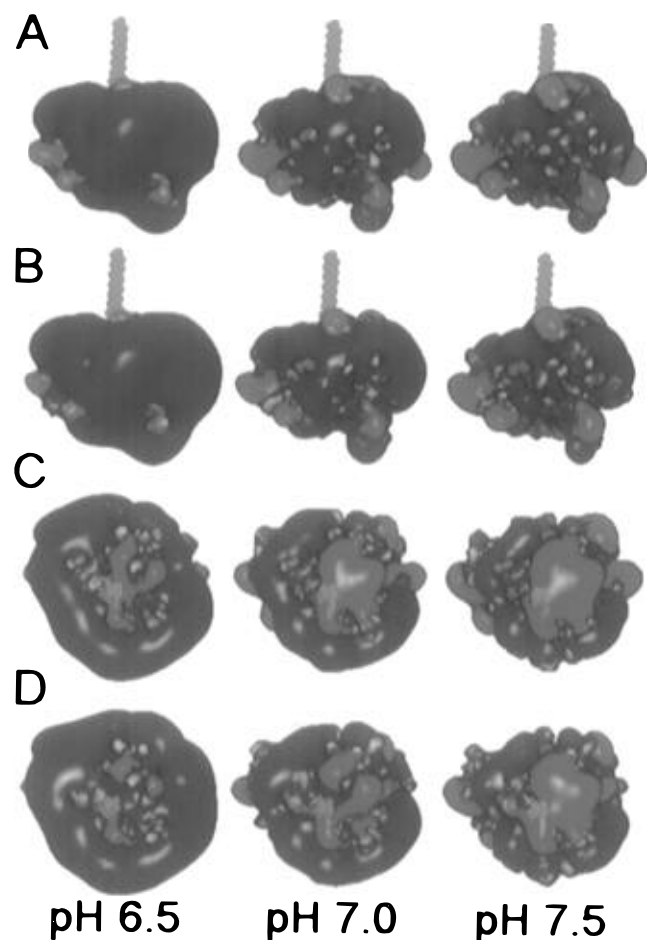


FIGURE 5: Molecular models of HsI (A and C) and HsII (B and D) built on the basis of the NMR data of recombinant HsI (Habazettl et al., 1992). An extended myristoyl chain (green) was attached at Gly<sup>2</sup> in both molecules. The electrostatic fields of HsI and HsII calculated on the basis of the theory of Poisson–Boltzmann are displayed as isocharge surfaces of  $+1kT/e$  (blue areas) and  $-1kT/e$  (red areas), where  $kT$  is the thermal energy and  $e$  is the elementary charge. Panels: side view (A and B); top view (C and D).

6A). At physiological salt concentrations, the charged residues localized within the Debye range of 1 nm can be assumed to interact with the membrane surface (McLaughlin, 1989). For HsI (HsII), the charged amino acid residues in this range are three lysines (one arginine and two lysines), seven (nine) histidines, and four (four) glutamic acids. Figure 6B shows the top view of the membrane contact region (dark area). The area requirement of the charged residues interacting with the lipid membrane can be estimated as  $\sim 300 \text{ \AA}^2$  from Figure 6B.

*Net Charge of Hisactophilins and of their Membrane Contact Region as a Function of the pH.* Figure 7 shows the calculated net charge of HsI and HsII as a function of the pH (see Materials and Methods). The titration curves of HsI (HsII) deviate only slightly from each other, and the calculated isoelectric points are 7.3 (7.5) for HsI (HsII), in perfect agreement with the measured isoelectric points (Hanakam et al., 1995).

The titration curves for the amino acid residues in the membrane contact region of HsI (HsII) are included in Figure 7. The net charge of the membrane binding region changes from  $+3.4$  ( $+4.9$ ) at pH 6.0 to  $-1.4$  ( $-1.2$ ) at pH 7.5 for HsI (HsII), and the respective isoelectric points are (6.9 and 7.1) in good agreement with the present experiments (Figure 4).

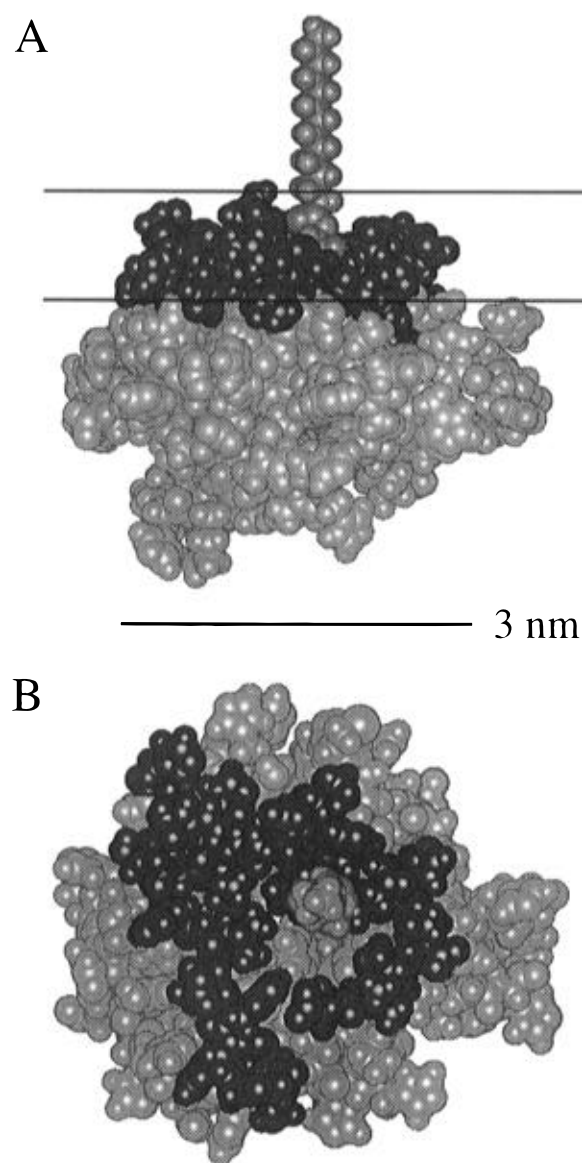


FIGURE 6: (A) Side view of the molecular model of HsI. The charged N- and C-terminal amino acid residues located within a range of 1 nm from the membrane surface (Debye range, indicated by the two parallel lines) have a potential to interact with the negatively charged membrane surface and are indicated in black. (B) Top view of the charged amino acid residues constituting the electrostatic binding region of HsI.

The good agreement between measured and calculated isoelectric points shows that this simple approach of calculating the net charge from the individual amino acid residues is reasonable for hisactophilins.

## DISCUSSION

The CD spectra of HsI and HsII isolated from *D. discoideum* were simulated on the basis of the NMR structure of HsI, assuming 57%  $\beta$ -sheet, 21%  $\beta$ -turn, and 22% random coil (Habazettl et al., 1992). The excellent agreement between experiment and simulation (Figure 1) provides evidence that the secondary structures of myristoylated HsI and HsII are similar to the structure of the unmyristoylated HsI. The NMR structure of the unmyristoylated HsI is therefore used as a molecular frame in which the present results can be visualized.

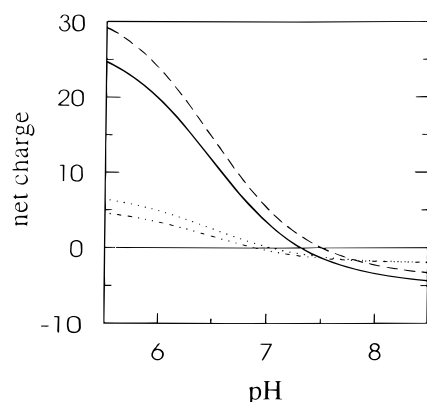


FIGURE 7: Calculated net charge (cf. Materials and Methods) of HsI (—) and HsII (---) and of the electrostatic binding region of HsI (— · —) and HsII (····) plotted as a function of the pH.

From monolayer expansion measurements, the extent of penetration of the hydrophobic and the electrostatic binding regions of hisactophilins into the lipid membrane can be deduced. The hisactophilin penetration area for electrically neutral POPC is  $A_p = 44 \pm 6 \text{ \AA}^2$ . For negatively charged POPC/POPG (75/25 mole/mole) monolayers, at a lateral packing density corresponding to that of a lipid bilayer,  $A_p$  is practically identical. The penetration area is thus on the same order of magnitude as that determined for myristic acid ( $A_p = 25 \text{ \AA}^2$ ) under similar conditions (Boguslavsky et al., 1994) and suggests that the relative area increase,  $\Delta A/A$ , is primarily due to the insertion of the myristoyl moiety with only a small contribution from amino acid side chains.

The free energy contributions of the hydrophobic and of the electrostatic binding regions to the overall binding constant of hisactophilins can be quantified as follows. The hydrophobic interaction of hisactophilins is characterized by a partition coefficient of  $K_A = (1.1 \pm 0.2) \times 10^4 \text{ M}^{-1}$  as deduced from binding measurements to neutral lipid monolayers at 32 mN/m. This value is virtually identical to the partition coefficient of  $10^4 \text{ M}^{-1}$  reported for the binding of small myristoylated model peptides to electrically neutral lipid bilayers (Peitsch & McLaughlin, 1993; Silvius & l'Heureux, 1994; Buser et al., 1994) and supports the conclusion that myristic acid penetration is the main hydrophobic interaction in hisactophilin binding. Direct proof for the insertion of a myristoyl moiety into the lipid membrane was obtained by means of photolabeling experiments of MARCKS and a MARCKS-related protein (MRP) (Vergères et al., 1995). The partition coefficient for the insertion of the myristoyl moiety into the lipid membrane of sucrose-loaded vesicles was, however, smaller by almost 2 orders of magnitude.

The electrostatic energy contribution can be estimated from the binding of hisactophilins to negatively charged lipid vesicles. At pH 6.0, the binding constant of hisactophilins to POPC/POPG (75/25 mole/mole) vesicles was determined as  $K_{app} = (8 \pm 1) \times 10^5 \text{ M}^{-1}$ . The incorporation of 25% of acidic lipids into the POPC membranes thus increased the binding constant by almost 2 orders of magnitude. Since the free energies of hydrophobic and electrostatic interactions

are additive, the overall partition coefficient,  $K_{app}$ , can be separated into the hydrophobic partition coefficient,  $K_A$ , for insertion of the myristoyl moiety into the membrane, and the electrostatic contribution,  $K_B^3$

$$K_{app} = K_A K_B \quad (6)$$

With the experimentally determined binding constants,  $K_{app} = (8 \pm 1) \times 10^5 \text{ M}^{-1}$  and  $K_A = (1.1 \pm 0.2) \times 10^4 \text{ M}^{-1}$ , the electrostatic binding region contributes a factor of  $K_B \cong 80$  at pH 6.0. This shows that the electrostatic contribution at physiological ion concentrations ( $\sim 154 \text{ mM NaCl}$ ) is rather small compared to the hydrophobic contribution, even at a low pH where the protein carries its maximum charge. This is in contrast to measurements with negatively charged lipid monolayers at low ionic strengths (20 mM NaCl) and at low surface pressures (25 mN/m) (Behrisch et al., 1995). The myristoylated and unmyristoylated HsII showed similar binding constants, suggesting that under these conditions the electrostatic interaction was the driving force for the binding of both proteins. This result can be traced back to the less efficient screening of electrostatic interactions at 20 mM NaCl compared to the physiological salt concentration employed in the present study.

The partition coefficients can be translated into free energies of binding,  $\Delta G$ , according to

$$\Delta G = -RT \ln(55.5 K_{app}) \quad (7)$$

where the factor 55.5 accounts for the cratic contribution and  $RT$  is the thermal energy. Hydrophobic binding alone yields  $\Delta G = -7.8 \text{ kcal/mol}$ , and hydrophobic binding and electrostatic binding together lead to  $\Delta G = -10.5 \text{ kcal/mol}$ . The contribution of the electrostatic term is thus  $-2.7 \text{ kcal/mol}$  at pH 6.0. Since hisactophilin binding to negatively charged membranes gave rise to an endothermic reaction enthalpy of  $\Delta H = +2.3 \text{ kcal}$  (Figure 3) and since  $\Delta G = \Delta H - T\Delta S$ , it can be concluded that the entropy is the driving force of the membrane binding reaction. This result is consistent with previous measurements which showed that the penetration of myristate into a lipid membrane is also entropy-driven (Peitsch & McLaughlin, 1993). In addition, the adsorption of pentyllysine to the membrane surface which mimics to a certain extent the adsorption of the electrostatic binding region of hisactophilins to the membrane surface is also endothermic (Montich et al., 1993).

Of particular relevance for the biological function of hisactophilins is the variation of the binding energy with the charge of the electrostatic binding region. We have therefore calculated the variation of the electric charge of the binding site (as described in Materials and Methods). The net charge of the binding region of HsI (HsII) changes from +3.4 (+4.9) at pH 6.0 to  $-1.4$  ( $-1.2$ ) at pH 7.5 (Figure 7) which is essentially due to a large number of histidine residues with a  $pK$  of 6.5 (Bull, 1971). An increase in pH is therefore expected to drastically reduce hisactophilin binding to negatively charged lipid membranes. This was indeed demonstrated by measuring the penetration of the electrostatic binding region into the head group region of a loosely packed POPC/POPG (75/25 mole/mole) monolayer at 22 mN/m as seen in Figure 4. Penetration of the electrostatic binding region was large at low pH and disappeared at pH  $7.0 \pm 0.1$ , where the equimolar mixture used in this experiment reaches its isoelectric point (cf. Figure 7).

<sup>3</sup> The synergistic interaction between the electrostatic and the hydrophobic binding motif of Src and MARCKS was described by a similar model, assuming that the hydrophobic and the electrostatic binding sites are in different locations, joined by a thin, electrically neutral flexible string (Buser et al., 1994; Kim et al., 1994a).

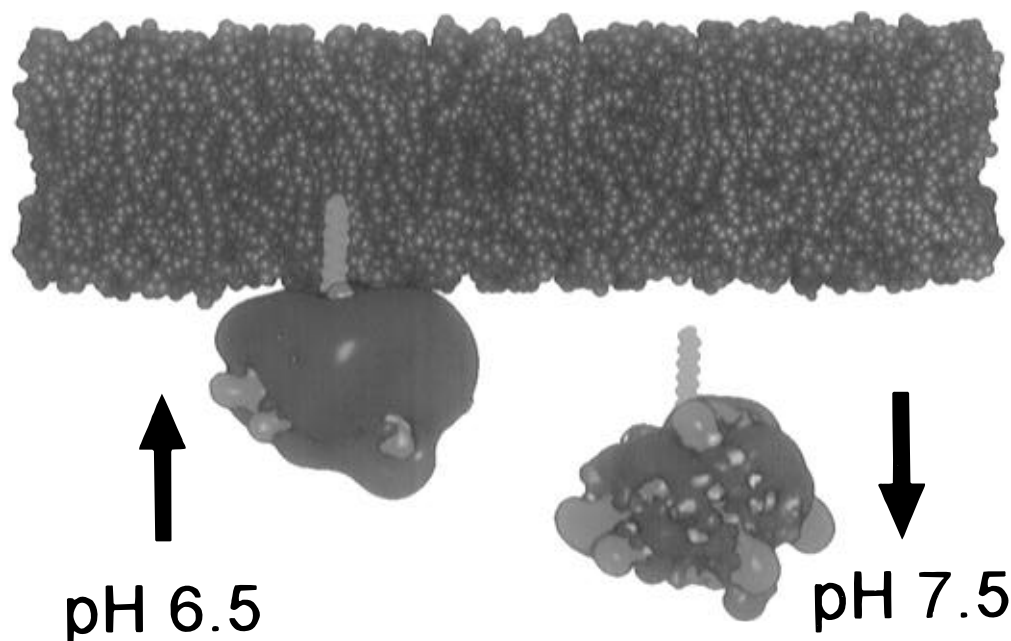


FIGURE 8: Representation of the pH-dependent membrane association of HsI. HsI was modeled using the NMR data (Habazettl et al., 1992), and isocharge surfaces of  $+1kT/e$  and  $-1kT/e$  are shown in blue and red, respectively. The lipid membrane was modeled using the parameters of molecular dynamics calculations (Heller et al., 1993). The arrows indicate the electrostatic attraction of HsI to the negatively charged membrane surface at pH 6.5 and the electrostatic repulsion at pH 7.5.

A pH shift to slightly basic values produces an electrostatic repulsion. Under these conditions, the apparent binding constant is reduced to the order of  $K_{app} \approx 10^3 \text{ M}^{-1}$  compared to  $K_{app} = (8 \pm 1) \times 10^5 \text{ M}^{-1}$  at pH 6. Even though the electrostatic contribution to the overall binding constant is modest under physiological conditions, this result shows that a small change in pH alters the partition between free and membrane-bound hisactophilin by three orders of magnitude, in agreement with results obtained *in vivo* (Hanakam et al., 1996). Our results are summarized in Figure 8 which shows molecular models of hisactophilin-lipid interactions at two different pH values, pH 6.5 and 7.5. These values are within the range of pH changes observed in living cells (Gross et al., 1983; Van Duijn & Inouye, 1991; Simchowitz & Cragoe, 1986). Under acidic conditions, the cluster of charged residues arranged around the myristoyl moiety is cationic (shown in blue) and is attracted to the negatively charged membrane surface, thereby enhancing the hydrophobic interaction of the myristoyl moiety. Under basic conditions the cluster of charged residues is overall anionic (shown in red) and is repelled from the membrane surface. The electrostatic binding region thus functions as a highly pH sensitive switch for reversibly binding hisactophilin to the plasma membrane.

In contrast to that of other myristoylated proteins (McLaughlin & Aderem, 1995), phosphorylation seems thus not to be necessary for the reversible binding of hisactophilins to the negatively charged plasma membrane. Nevertheless, phosphorylation does occur *in vivo* (Hanakam et al., 1995) and might function as an additional regulatory element either for membrane binding or for actin binding. Since the putative phosphorylation site is not located in the membrane binding region, the latter possibility seems more plausible. It has been shown previously that HsI binds to actin at pH  $< 7.2$  and unbinds at pH  $> 7.2$  (Scheel et al., 1989). These earlier data in combination with the present results suggest that

hisactophilins act as pH-regulated linkers between actin and the plasma membrane.

#### ACKNOWLEDGMENT

We thank Dr. Tadeusz Holak for providing the structural data of hisactophilin (HsI), Dr. Helmut Heller for providing the data for the simulation of the lipid bilayer, Dr. Eveline Terzi for simulating the CD spectra, and Dr. Joachim Seelig for critically reading the manuscript.

#### REFERENCES

- Behrisch, A., Dietrich, C., Noegel, A. A., Schleicher, M., & Sackmann, E. (1995) *Biochemistry* 34, 15182–15190.
- Beschiaschvili, G., & Seelig, J. (1992) *Biochemistry* 31, 10044–10053.
- Bigay, J., Faurobert, E., Franco, M., & Chabre, M. (1994) *Biochemistry* 33, 14081–14090.
- Blenis, J., & Resh, M. D. (1993) *Curr. Opin. Cell Biol.* 5, 984–989.
- Blume, A. (1979) *Biochim. Biophys. Acta* 557, 32–44.
- Boguslavsky, V., Rebecchi, M., Morris, A. J., Jhon, D.-Y., Rhee, S. G., & McLaughlin, S. (1994) *Biochemistry* 33, 3032–3037.
- Bull, H. B. (1971) *An Introduction to Physical Biochemistry*, 2nd ed., Davis, Philadelphia.
- Buser, C. A., Sigal, C. T., Resh, M. D., & McLaughlin, S. (1994) *Biochemistry* 33, 13093–13101.
- Demel, R. A., Geurts van Kessel, W. S. M., Zwaal, R. F. A., Roelofsen, B., & van Deenen, L. M. (1975) *Biochim. Biophys. Acta* 406, 97–107.
- Devereux, J., Haerberli, P., & Smithies, O. (1984) *Nucleic Acids Res.* 12, 387–395.
- Evans, R. W., Williams, M. A., & Tinoco, J. (1987) *Biochem. J.* 245, 455–462.
- Fromherz, P. (1975) *Rev. Sci. Instrum.* 46, 1380–1385.
- Gross, J. D., Bradbury, J., Kay, R. R., & Peacey, M. J. (1983) *Nature* 303, 244–245.
- Habazettl, J., Gondol, D., Wilschek, R., Otlewski, J., Schleicher, M., & Holak, T. A. (1992) *Nature* 359, 855–858.
- Hanakam, F., Eckerskorn, C., Lottspeich, F., Müller-Taubenberger, A., Schäfer, W., & Gerisch, G. (1995) *J. Biol. Chem.* 270, 596–602.



- Hanakam, F., Albrecht, R., Eckerskorn, C., Matzner, M., & Gerisch, G. (1996) *EMBO J.* 15, 2935–2943.
- Heller, H., Schaefer, M., & Schulten, K. (1993) *J. Phys. Chem.* 97, 8343–8360.
- Kim, J., Blackshear, P. J., Johnson, J. D., & McLaughlin, S. (1994a) *Biophys. J.* 67, 227–237.
- Kim, J., Shishido, T., Jiang, X., Aderem, A., & McLaughlin, S. (1994b) *J. Biol. Chem.* 269, 28214–28219.
- Magee, A. I., & Courtneidge, S. A. (1985) *EMBO J.* 4, 1137–1144.
- McLaughlin, S. (1989) *Annu. Rev. Biophys. Chem.* 18, 113–136.
- McLaughlin, S., & Aderem, A. (1995) *TIBS* 20, 272–277.
- Montich, G., Scarlata, S., McLaughlin, S., Lehmann, R., & Seelig, J. (1993) *Biochim. Biophys. Acta* 1146, 17–24.
- Op den Kamp, J. A. F. (1979) *Annu. Rev. Biochem.* 48, 47–71.
- Peitzsch, R. M., & McLaughlin, S. (1993) *Biochemistry* 32, 10436–10443.
- Scheel, J., Ziegelbauer, K., Kupke, T., Humbel, B. M., Noegel, A. A., Gerisch, G., & Schleicher, M. (1989) *J. Biol. Chem.* 264, 2832–2839.
- Seelig, A. (1987) *Biochim. Biophys. Acta* 1030, 111–118.
- Seelig, A. (1992) *Biochemistry* 31, 2897–2904.
- Seelig, A., & Macdonald, P. M. (1989) *Biochemistry* 28, 2490–2496.
- Seelig, A., Alt, T., Lotz, S., & Hölzemann, G. (1996) *Biochemistry* 35, 4365–4374.
- Sigal, C. T., Zhou, W., Buser, C. A., McLaughlin, S., & Resh, M. D. (1994) *Proc. Natl. Acad. Sci. U.S.A.* 91, 12253–12257.
- Silvius, J. R., & l'Heureux, F. (1994) *Biochemistry* 33, 3014–3022.
- Simchowicz, L., & Cragoe, E. J., Jr. (1986) *J. Biol. Chem.* 261, 6492–6500.
- Taschner, N. (1992) Diploma Thesis, University of Basel, Basel, Switzerland.
- Van Duijn, B., & Inouye, K. (1991) *Proc. Natl. Acad. Sci. U.S.A.* 88, 4951–4955.
- Van Lookeren Campagne, M. M., Aerts, R. J., Spek, W., Firtel, R. A., & Schaap, P. (1989) *Development* 105, 401–406.
- Vergères, G., Manenti, S., Weber, T., & Stürzinger, C. (1995) *J. Biol. Chem.* 270, 19879–19887.
- Wiseman, T., Williston, S., Brandts, J. F., & Lin, L.-N. (1989) *Anal. Biochem.* 179, 131–137.
- Yang, J. T., Wu, C.-S. C., & Martinez, H. M. (1986) *Methods Enzymol.* 130, 208–269.

BI960789J